

Effect of Wavelength on the Photocurrent and Photovoltage of Vertical Parallel Silicon Solar Cells under Steady State Condition

Gökhan Sahin

Electric and Electronic Engineering Department, IĞDIR University, Iğdır 76000, Turkey
g.sahin38@hotmail.fr

Abstract-The effect of wavelength on the photocurrent and photovoltage of a vertical parallel junction solar cell under steady state condition was theoretically analyzed. Based on the diffusion equation, the excess minority carrier's density is expressed; both photocurrent density and photovoltage determine the junction recombination velocity and the wavelengths. The excess minority carrier density, the photocurrent density, and the photovoltage were calculated and plotted. The objective of this work is to show the effects of solar cell junction recombination velocity and the wavelengths on these electrical parameters. We have shown the effect of wavelength on initiating the short-circuit (Sf_{sc}) and limited the open circuit (Sf_{oc}) of the solar cell through the junction recombination velocity. The determination of Sf_{oc} obtained from the curve of photovoltage versus Sf , and the determination of Sf_{sc} is through from the curve of the photocurrent density according to Sf .

Keywords- Vertical Parallel Solar Cell; Recombination Velocity; Photocurrent; Photovoltage

I. INTRODUCTION

The improvement of the solar cells limits the recombination of the excess minority carrier's photogenerated. Parameters and the control of the technological process of manufacturing are significant during the conception of these devices. Several methods of characterization in static or quasi-static mode, as well as in transient state and dynamic frequency mode have been developed for the determination of one or several parameters [1, 2]. In this regard, we resolve continuity equation about relative to excess minority carriers in the base.

Ever since the reporting of the first silicon solar cells [3, 4], a lot of research work has been done on these cells during the last few decades [5-8]. Efforts have been made to improve the efficiency of the solar cells and various modified structures have developed, which resulted in improved efficiency. This efficiency depends on several phenomenological parameters, the diffusion length (L), the diffusion coefficient (D), the junction recombination velocity (Sf), the reflexion coefficient (R) and the absorption coefficient (α) [9, 10]. Consequently, several methods were developed for the determination of these parameters.

In this work, we present a method of junction recombination velocity determination initiating the short-circuit (Sf_{sc}) and limiting the open circuit (Sf_{oc}) for a solar cell. The study will be done primarily in the base because the contribution of the transmitter is negligible.

II. THEORY

Let us consider a silicon solar cell with parallel vertical junction N + P doped in Fig. 1:

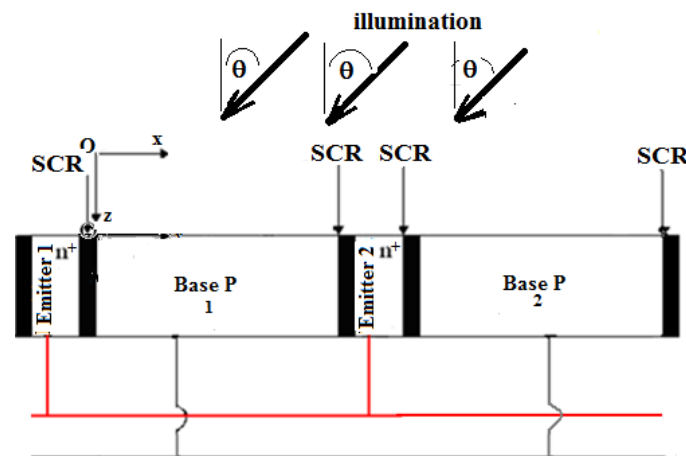


Fig. 1 Vertical parallel junction silicon solar cell

This photovoltaic cell includes three parts:

- i. Emitter: frontal zone of N + type, it is doped with donor atoms.
- ii. Base: zone of P type, it is doped with acceptor atoms.
- iii. SCR: we find it between the emitter and the base, and there reigns an intrinsic electrical field (E) which separates the electron-hole pairs.

When the solar cell illuminates under the incidence angle (θ), there is a creation of electron-hole pairs in the base.

Given that the contribution of the base to the photocurrent is larger than that of the emitter [10], our analysis will only be developed in the base region.

Taking into account the generation, recombination and diffusion phenomena in the base, the continuity equation is given by the following equation [11-14]:

$$D(\omega) \cdot \frac{\partial^2 \delta(x, \theta, t)}{\partial x^2} - \frac{\delta(x, \theta, t)}{\tau} = -G(z, \theta, t) + \frac{\partial \delta(x, \theta, t)}{\partial t} \quad (1)$$

$D(\omega)$ [15] and τ are respectively, the excess minority carrier's diffusion constant and lifetime.

The excess minority carriers' density written as:

$$\delta(x, t) = \delta(x) \exp(-j\omega t) \quad (2)$$

Carrier generation rate $G(z, \theta, t)$ is given by:

$$G(z, \theta, \lambda, t) = g(z, \theta, \lambda) \exp(-j\omega t) \quad (3)$$

Where

$$g(z, \theta, \lambda) = \alpha(\lambda)(1 - R(\lambda)) \cdot \phi(\lambda) \cdot \exp(-\alpha(\lambda) \cdot z) \cdot \cos(\theta) \quad (4)$$

H is the base width, θ is the illumination incidence angle, x is the depth in the base, ω is the angular frequency, and z is the base depth according to the vertical axis and λ the illumination wavelength.

If we replace Eq. (2) into Eq. (1), the temporary part is eliminated, and we obtain:

$$\frac{\partial^2 \delta(x)}{\partial x^2} - \frac{\delta(x, \theta, t)}{L(\omega)^2} = -\frac{g(z, \theta)}{D(\omega)} \quad (5)$$

The solution of this equation is:

$$\delta(x, \omega, \theta, z, Sf, \lambda) = A \cosh\left(\frac{x}{L(\omega)}\right) + B \sinh\left(\frac{x}{L(\omega)}\right) + \frac{L(\omega)^2}{D(\omega)} \cdot \alpha(\lambda)(1 - R(\lambda)) \cdot \phi(\lambda) \cdot \exp(\alpha(\lambda) \cdot z) \cdot \cos(\theta) \quad (6)$$

Coefficients A and B are determined by the following boundary conditions [16]:

- **at the junction ($x = 0$):**

$$D(\omega) \cdot \frac{\partial \delta(x, \omega, \theta)}{\partial x} \Big|_{x=0} = Sf \cdot \delta(x, \omega, \theta) \Big|_{x=0} \quad (7)$$

Sf is the excess minority carrier's recombination velocity at each junction [17].

- **at the middle of the base ($x = H/2$):**

$$D(\omega) \cdot \frac{\partial \delta(x, \omega, \theta)}{\partial x} \Big|_{x=H/2} = 0 \quad (8)$$

The excess minority carriers in the base will flow to the two junctions by diffusion, the photocurrent, and photovoltage density.

III. RESULTS AND DISCUSSION

A. Profile of Excess Minority Carrier's Density

The figure gives the profile of the excess minority carrier's density, Fig. 2(a) and Fig. 2(b).

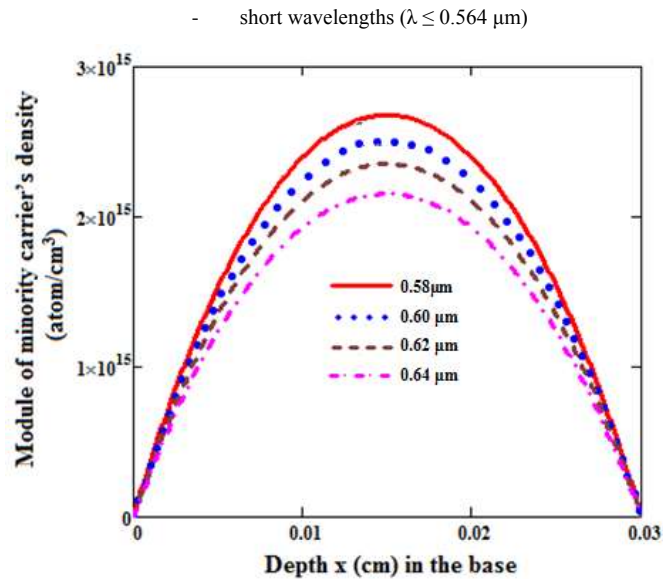


Fig. 2(a) Excess minority carrier's density versus depth x in the base for various short wavelengths

$L_0 = 0.0001 \text{ cm}$, $D_0 = 26 \text{ cm}^2/\text{s}$, $Sf = 3.10^3 \text{ cm/s}$, $H = 0.03 \text{ cm}$, $z = 0.0001 \text{ cm}$. 1: $\lambda = 0.58 \mu\text{m}$; 2: $\lambda = 0.60 \mu\text{m}$; 3: $\lambda = 0.62 \mu\text{m}$; 4: $\lambda = 0.64 \mu\text{m}$

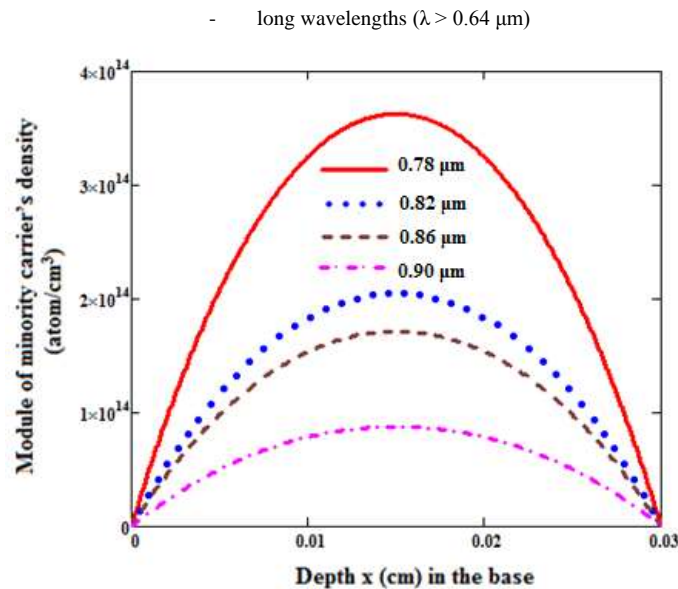


Fig. 2(b) Excess minority carrier's density versus depth x in the base for various long wavelengths

$L_0 = 0.0001 \text{ cm}$, $D_0 = 26 \text{ cm}^2/\text{s}$, $Sf = 3.10^3 \text{ cm/s}$, $H = 0.03 \text{ cm}$, $z = 0.0001 \text{ cm}$. 1: $\lambda = 0.58 \mu\text{m}$; 2: $\lambda = 0.60 \mu\text{m}$; 3: $\lambda = 0.62 \mu\text{m}$; 4: $\lambda = 0.64 \mu\text{m}$

For a given wavelength, the curve presents three parts:

The density of the excess minority carrier's increases until reaching a maximum, which corresponds to a depth x_0 , in the base, beyond the value x_0 the excess minority carrier's density decreases.

Thus we distinguish two zones: The zone corresponding to the increase of the minority carrier's density to the active gradient: that is due to the crossing of the minority carrier's charge to the junction which takes part in the photocurrent [18].

The zone corresponding to the reduction in the excess minority carrier's density to the negative gradient; the minority carrier's frequently undergo in depth and the surface recombination. The maximum corresponds to the null angle, which indicates storage of carrier's density.

It is seen that for the short wavelength (λ) values; absorption is done close to the junction, whereas for the long wavelengths values, absorption moves in depth x.

The expression of the excess minority carrier's density enables us to obtain that the photocurrent density starting from the relation of Fick. This is undoubtedly an advantage of vertical parallel junction solar cells. We can also observe a decrease of the excess minority carrier density for the chosen wavelength as seen with the other parameters [19].

B. Photocurrent Density

The photocurrent density gives the following expression (9) [10, 19, 20]:

$$J_{ph} = 2 \cdot q \cdot D(\omega) \cdot \left. \frac{\partial \delta(x, \omega, \theta)}{\partial x} \right|_{x=0} \tag{9}$$

Based on the density of excess minority carriers created in the base of the solar cell, we established the photocurrent density of carriers by the Fick equation [21-24].

Where q is the elementary charge ($q = 1.6 \cdot 10^{-19}$ C).

A plot of the photocurrent density versus junction recombination velocity for various wavelengths is present on Fig. 3(a) and Fig. 3(b).

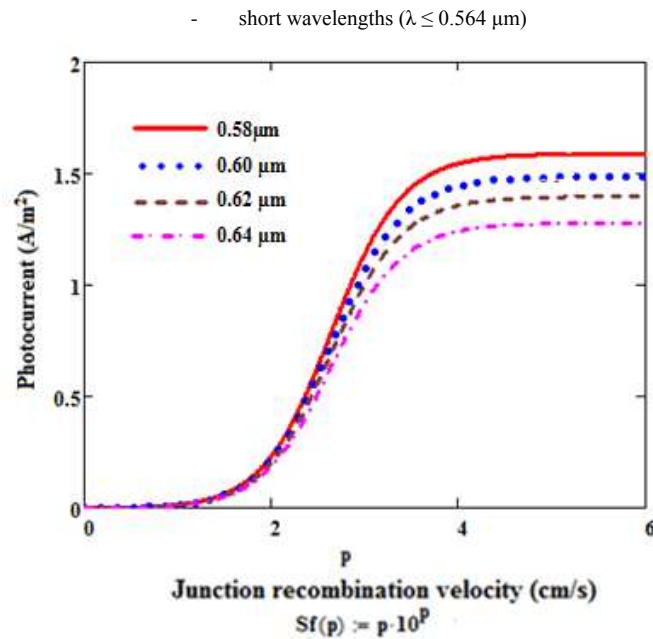


Fig. 3(a) Photocurrent density versus the junction recombination versus for various short wavelengths

$L_0 = 0.0001$ cm, $D_0 = 26$ cm²/s, $Sf = 3 \cdot 10^3$ cm/s, $H = 0.03$ cm, $z = 0.0001$ cm. 1: $\lambda = 0.58 \mu\text{m}$; 2: $\lambda = 0.60 \mu\text{m}$; 3: $\lambda = 0.62 \mu\text{m}$; 4: $\lambda = 0.64 \mu\text{m}$

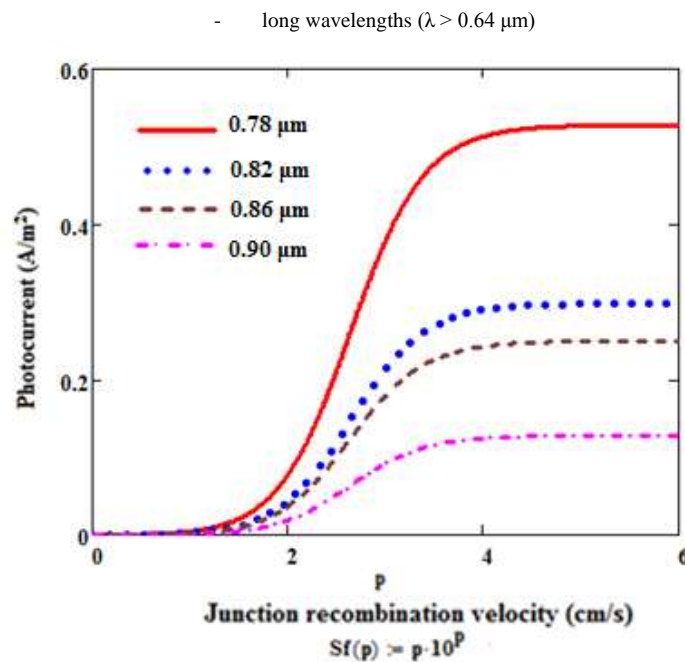


Fig. 3(b) Photocurrent density versus the junction recombination versus for various wavelengths

$L_0 = 0.0001$ cm, $D_0 = 26$ cm²/s, $Sf = 3 \cdot 10^3$ cm/s, $H = 0.03$ cm, $z = 0.0001$ cm. 1: $\lambda = 0.58 \mu\text{m}$; 2: $\lambda = 0.60 \mu\text{m}$; 3: $\lambda = 0.62 \mu\text{m}$; 4: $\lambda = 0.64 \mu\text{m}$

We present at Fig. 3(a) and Fig. 3(b) the profile of the photovoltage versus junction recombination velocity for different wavelength values. These figures allow observing an increase in photocurrent density with the junction recombination velocity [24-27]; the photocurrent density reaches a maximum where it varies microscopic with the junction recombination velocity. Indeed, since the junction recombination velocity reflects the flow of carriers across the junction [11, 15, 18, 19], increasing the junction recombination velocity means to increase the movement of carriers through the terminal and a larger collection of carriers. In other words, it is thus an increase in the current density.

The flow of carriers across the junction reaches a limit for this time thereby characterizing the operation in short-circuiting of the solar cell. A little load resistor requires the movement of a large current and therefore requires a high junction recombination velocity (short-circuit situation). When the load resistance is high, little current flows through the burden, and the movement of carriers across the junction is small. That is to say that the junction recombination velocity is low (open-circuit situation).

Junction recombination velocity is the phenomenological equivalent to the external load, which itself is macroscopic; these two factors, describe the same operating conditions of the solar cell as we have seen.

C. Photovoltage Density

According to the Boltzmann relation, the photovoltage is obtained by the expression (10) [1, 27].

$$V_{ph} = V_T \cdot \ln \left[1 + \frac{N_b}{n_0} \cdot \delta(0) \right] \quad (10)$$

with

$$V_T = \frac{K \cdot T}{q} \quad (11)$$

V_T the thermal voltage, N_b the base doping density, N_i is the intrinsic carrier density, n_0 is the carrier's density at equilibrium.

We present at Fig. 4(a) and Fig. 4(b) the profile of the photovoltage versus junction recombination velocity for different wavelength values:

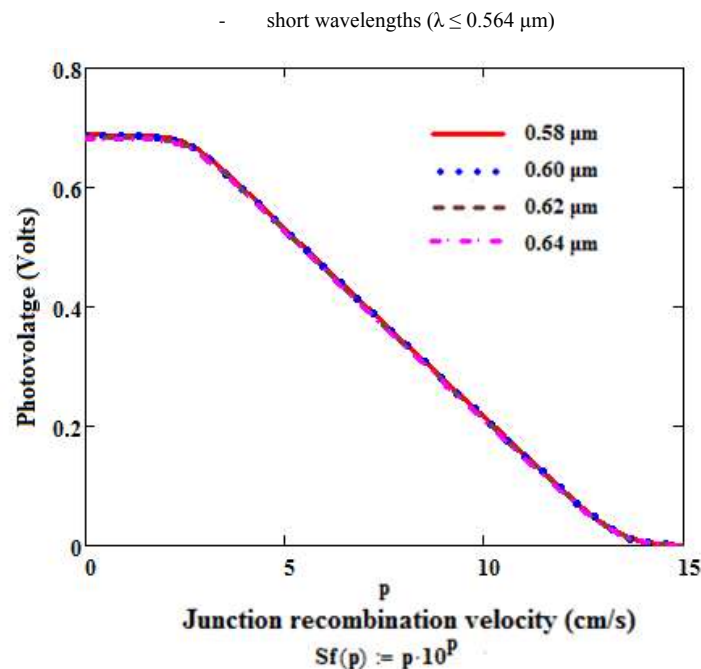


Fig. 4(a) The module of the photovoltage versus the logarithm of the frequency for various short wavelengths

$L_0 = 0.0001 \text{ cm}$, $D_0 = 26 \text{ cm}^2/\text{s}$, $Sf = 3 \cdot 10^5 \text{ cm/s}$, $H = 0.03 \text{ cm}$, $z = 0.0001 \text{ cm}$. 1: $\lambda = 0.58 \mu\text{m}$; 2: $\lambda = 0.60 \mu\text{m}$; 3: $\lambda = 0.62 \mu\text{m}$; 4: $\lambda = 0.64 \mu\text{m}$

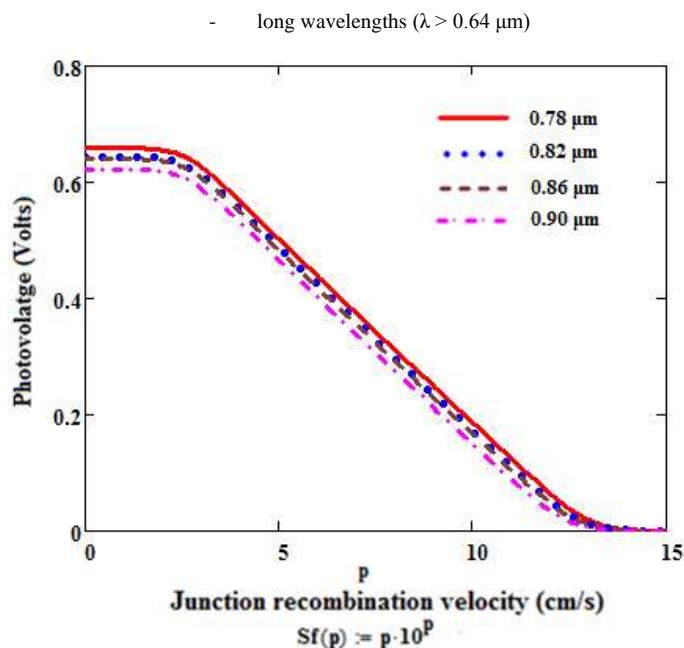


Fig. 4(b) The module of the photovoltage versus the logarithm of the frequency for different long wavelengths values

$L_0 = 0.0001 \text{ cm}$, $D_0 = 26 \text{ cm}^2/\text{s}$, $Sf = 3.10^3 \text{ cm/s}$, $H = 0.03 \text{ cm}$, $z = 0.0001 \text{ cm}$. 1: $\lambda = 0.58 \mu\text{m}$; 2: $\lambda = 0.60 \mu\text{m}$; 3: $\lambda = 0.62 \mu\text{m}$; 4: $\lambda = 0.64 \mu\text{m}$

We observe in this case that: For the small values of the junction recombination velocity, the maximum photovoltage solar cell is in the open-circuit situation. Whereas for the high values of the junction recombination velocity, the photovoltage decreases and tends towards zero: the solar cell is in short-circuit situation. The representation of the photocurrent density and that of the photovoltage versus the junction recombination velocity, give two stages in general corresponding to the operation of the solar cell in short-circuit or in an open circuit. Whereas for the high values of the junction recombination velocity, the photovoltage decreases and leans towards zero: the solar cell is in a situation of short-circuiting. The representation of the photocurrent density and that of the photovoltage versus the junction recombination velocity, give two stages in general corresponding to the operation of the solar cell in short-circuit or in open-circuit. For each stage, we can make corresponding values of junction recombination velocity (Sf) [15, 18, 19, 28]. What leads us to this work to propose a method of junction recombination velocity determination, initiating the short-circuit Sf_{sc} and limiting the open circuit Sf_{oc} .

D. Junction Recombination Velocity Determination Initiating the Short-circuit Sf_{sc} and Limiting the Open Circuit Sf_{oc}

1) Starting the Short-circuit Sf_{sc}

In Fig. 5(a) and Fig. 5(b), we represent the profile of the short-circuit photocurrent and photovoltage as a function of junction recombination velocity for different wavelengths values:

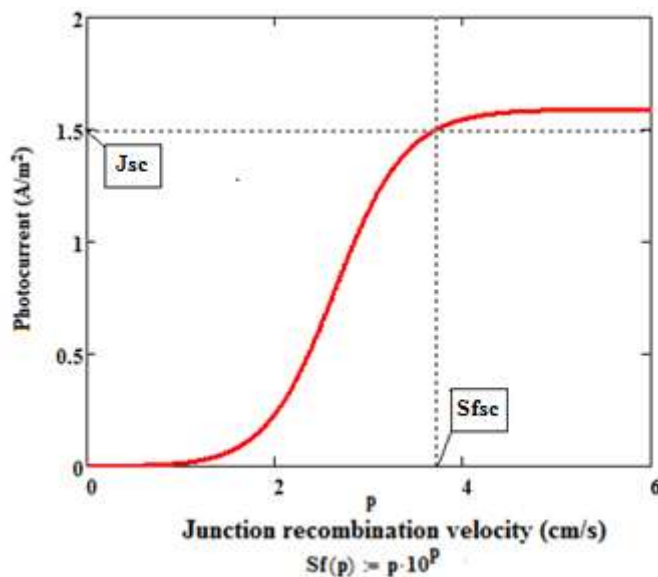


Fig. 5(a) Technique of determination of the photocurrent density for $\lambda=0.58 \mu\text{m}$

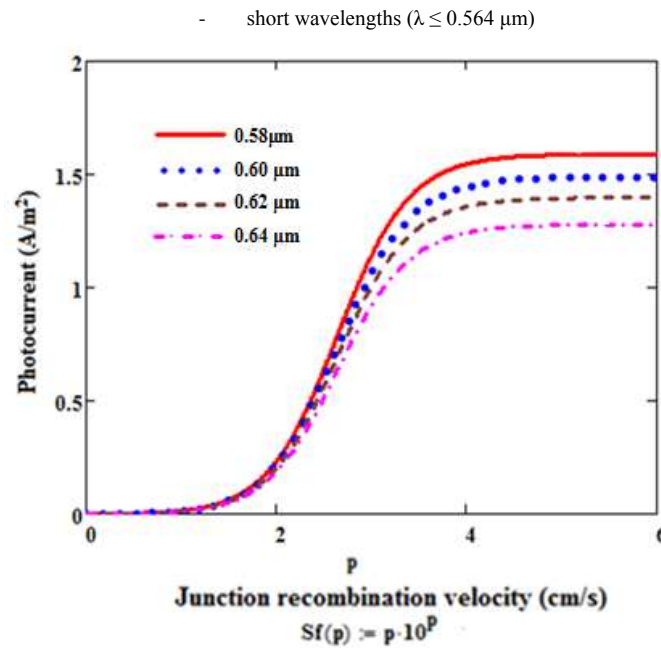


Fig. 5(b) Photocurrent density versus the junction recombination velocity for various short wavelengths

$L_0 = 0.0001 \text{ cm}$, $D_0 = 26 \text{ cm}^2/\text{s}$, $Sf = 3.10^3 \text{ cm/s}$, $H = 0.03 \text{ cm}$, $z = 0.0001 \text{ cm}$. 1: $\lambda = 0.58 \mu\text{m}$; 2: $\lambda = 0.60 \mu\text{m}$; 3: $\lambda = 0.62 \mu\text{m}$; 4: $\lambda = 0.64 \mu\text{m}$

The short-circuit maximum photocurrent density, remains almost constant for the low frequencies for $\log \omega < 4$. When the frequency becomes high ($\log \omega > 4$), the photocurrent decreases gradually toward zero. The amplitude of the photocurrent also decreases as a function of wavelength because little-photogenerated minority carriers across the junction due to the illumination of a portion of the surface of the solar cell [18]. The determination of (Sf_{sc}) consists in projecting the value of the photocurrent density of short-circuiting of the solar cell on the axis corresponding to the junction recombination velocity. The found value is the junction recombination velocity initiating the short-circuit for a given wavelength. The Fig. 5(a) confirms that.

The influence of the short wavelengths (λ) on the photocurrent density versus the junction recombination velocity shown in Fig. 5(b).

For short wavelengths in Fig. 5(b), the amplitude of the photocurrent increases with the short wavelengths. This is consistent with the fact that the generation of minority carriers is greater in the region close to the surface of the emitter and that the incident photons are abundant energy and then penetrate tiny in the semiconductor material. The surface diffusion, conduction interface, and the photocurrent density increased for short wavelengths [18].

The following tables (Table 1 and Table 2) represents various values of junction recombination velocity initiating the short-circuit for different short wavelengths values.

TABLE 1 JUNCTION RECOMBINATION VELOCITY IS STARTING THE CURRENT OF SHORT-CIRCUITS VERSUS SHORT WAVELENGTHS VALUES [29]

$J_{cc \text{ exp}} (\text{mA}/\text{cm}^2)$	$\lambda (\mu\text{m})$	$Sf_{cc} (\text{cm}/\text{s})$
0.0369	0.58	$4.7 \cdot 10^{4.7}$
0.0369	0.60	$4.9 \cdot 10^{4.9}$
0.0369	0.62	$5.1 \cdot 10^{5.1}$
0.0369	0.64	$5.5 \cdot 10^{5.5}$

TABLE 2 JUNCTION RECOMBINATION VELOCITY IS STARTING THE CURRENT OF OPEN-CIRCUIT VERSUS SHORT WAVELENGTHS VALUES [29]

$V_{oc} (\text{V}/\text{cm}^2)$	$\lambda (\mu\text{m})$	$Sf_{oc} (\text{cm}/\text{s})$
0.29	0.58	$3.22 \cdot 10^{3.22}$
0.29	0.60	$3.20 \cdot 10^{3.2}$
0.29	0.62	$3.12 \cdot 10^{3.12}$
0.29	0.64	$3.04 \cdot 10^{3.04}$

2) Limiting the Open-circuit Sf_{oc}

In Fig. 6(a) and Fig. 6(b), we represent the profile of the open circuit photovoltage and photovoltage as a function of junction recombination velocity for different wavelengths values:

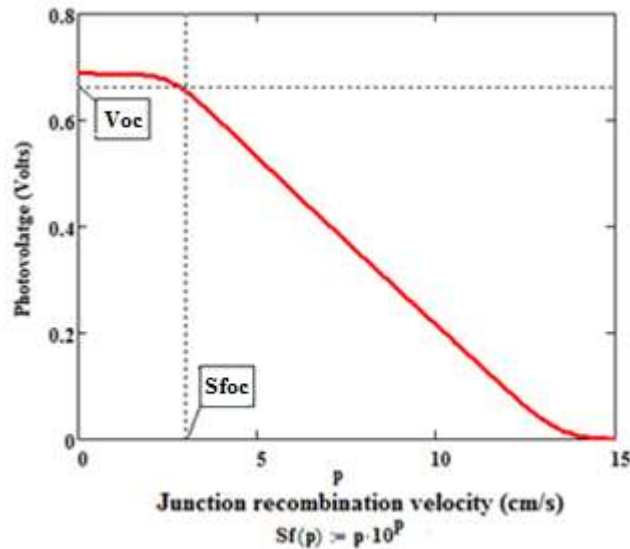


Fig. 6(a) Technique of junction recombination velocity determination beginning to the open circuit versus wavelength, $\lambda=0.58 \mu\text{m}$
 - short wavelengths ($\lambda \leq 0.64 \mu\text{m}$)

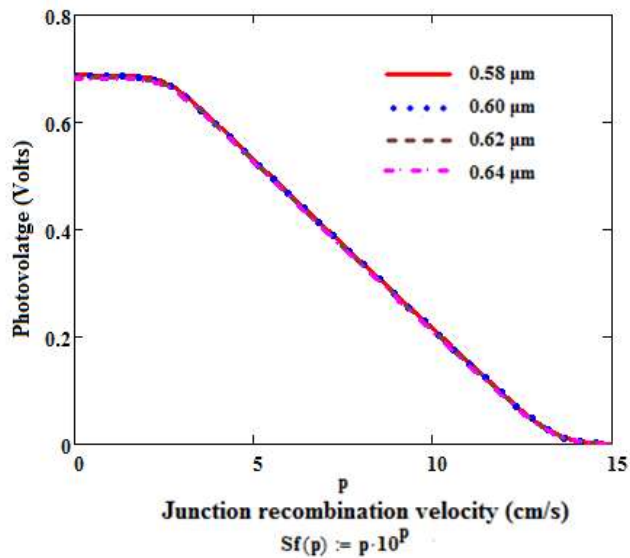


Fig. 6(b) The module of the photovoltage versus the logarithm of the frequency for various short wavelengths
 $L_0 = 0.0001 \text{ cm}$, $D_0 = 26 \text{ cm}^2/\text{s}$, $Sf = 3 \cdot 10^3 \text{ cm/s}$, $H = 0.03 \text{ cm}$, $z = 0.0001 \text{ cm}$. 1: $\lambda = 0.58 \mu\text{m}$; 2: $\lambda = 0.60 \mu\text{m}$; 3: $\lambda = 0.62 \mu\text{m}$; 4: $\lambda = 0.64 \mu\text{m}$

We proceed in the same way as previously for the junction recombination velocity determination beginning to the open circuit. In other words, the experimental value of the photovoltage of an open circuit is projected on the axis corresponding to the junction recombination velocity. The modulus of the open circuit photovoltage decreases when the junction recombination velocity is very high. In the area of the junction recombination velocity, the module opens the circuit photovoltage, a constant value for a value of the angle of short wavelength given well [18].

We proceed in the same way as previously for the junction recombination velocity determination beginning to the open-circuit. In other words, the value of the photovoltage of open-circuit is projected on the axis corresponding to the junction recombination velocity.

The photovoltage is maximum at low recombination speed at the junction. It decreases linearly to cancel the large recombination velocities. Next Planck's law, the wave does not have enough energy to generate minority carriers in depth. The phenomena of photo degeneration, dislocations, and manufacturing defects are all obstacles contributing to the decline in generation of carriers when working with long wavelengths [18].

IV. CONCLUSION

A theoretical study of a vertical junction solar cell is presented. Electrical parameters such as photocurrent density,

photovoltage have been determined, and shown the effects of solar cell. This study exhibits the fact that photocurrent density and photovoltage, depend on the solar cell. The excess minority charge carriers density in the base was determined and plotted versus base depth for different wavelengths values. The excess of the photovoltage and photocurrent deducted from the minority carrier's density and their profile depends upon the junction recombination velocity for various wavelengths values. This study confirms that by examining the electric power, it will undergo the effect of wavelengths. To use the junction recombination velocity, concept permits us to determine the solar cell's electric power for any operating point of the solar cell contrarily to other's studies; which used the maximal power point tracking (MPPT) control technic characterized by one operating point corresponding to the maximum output power delivered by the solar cell. The junction recombination velocity limiting the open circuit voltage and short circuit photocurrent determines the solar cell under different wavelengths values.

REFERENCES

- [1] G. Sahin, "Effect of wavelength on the electrical parameters of a vertical parallel junction silicon solar cell illuminated by its rear side in frequency domain," *Results in Physics*, vol. 6, pp. 107-111, March 2016.
- [2] J.W. Orton and P. Blood, *The Electrical Characterization of Semiconductor: Measurement of Minority Carrier Properties*, 13th ed., Academic Press, London, pp. 279-286, November 1990.
- [3] D.M. Chapin, C.S. Fuller, and G.L. Pearson, "A new silicon p-n junction photocell for converting solar radiation into electrical power," *J. Appl. Phys.*, vol. 25, pp. 676-677, May 1954.
- [4] M.B. Prince, "Silicon solar energy converters," *J. Appl. Phys.*, vol. 26, pp. 534-540, May 1955.
- [5] W. Shockley and H.J. Queisser, "Detailed balance limit of efficiency of p-n junction solar cell," *J. Appl. Phys.*, vol. 32, pp. 510-519, 1961.
- [6] M. Wolf, "A new look at silicon solar cell performance," *Energy Conversion*, vol. 11, pp. 63-73, 1971.
- [7] A.W. Blakers and M.A. Green, "20% efficiency silicon solar cells," *Appl. Phys. Lett.*, vol. 48, pp. 215-217, January 1986.
- [8] W. Wang, J. Zhao, and M.A. Green, "24% efficiency silicon solar cells," *Appl. Phys. Lett.*, vol. 57, pp. 602-604, August 1990.
- [9] M. M. Dione, S. Mbodji, M. L. Samb, M. Dieng, M. Thiame, S. Ndoeye, F. I. Barro, and G. Sissoko, "Junction Under Constant Multispectral Light: Determination Of Recombination Parameters," *24th European Photovoltaic Solar Energy Conference*, Hamburg, Germany, pp. 465-468, 21-25 September 2009.
- [10] G. Sahin, M. Dieng, M. A. O. E. Moujtaba, M. I. Ngom, A. Thiam, and G. Sissoko, "Capacitance of Vertical Parallel Junction Silicon Solar Cell under Monochromatic Modulated Illumination," *Journal of Applied Mathematics and Physics*, vol. 3, pp. 1536-1543, 2015.
- [11] N. Honma and C. Munakata, "Sample Thickness Dependence of Minority Carrier Lifetimes Measured Using an ac Photovoltaic Method," *Japanese Journal of Applied Physics*, vol. 26, no. 12, pp. 233-236, December 1987.
- [12] N. Honma, C. Munakata, and H. Shimizu, "Calibration of Minority Carrier Lifetimes Measured with an ac Photovoltaic Method," *Japanese Journal of Applied Physics*, vol. 27, no. 7, pp. 1322-1326, July 1988.
- [13] A. Mandelis, "Coupled ac photocurrent and photothermal reflectance response theory of semiconducting p-n junctions," *J. Appl. Phys.*, vol. 66, iss. 11, pp. 5572-5583, December 1989.
- [14] M. Sane, G. Sahin, F. I. Barro, and A. S. Maiga, "Incidence angle and spectral effects on vertical junction silicon solar cell capacitance," *Turk. J. Phys.*, vol. 38, pp. 221-227, June 2014.
- [15] H. L. Diallo, A. Wereme, A. S. Maiga, and G. Sissoko, "New approach of both junction and back surface recombination velocities in a 3D modelling study of a polycrystalline silicon solar cell," *Eur. Phys. J. Appl. Phys.*, vol. 42, pp. 203-11, June 2008.
- [16] A. Gover and P. Stella, "Vertical Multijunction Solar-Cell One-Dimensional Analysis," *IEEE Transactions on Electron Devices*, vol. 21, iss. 6, pp. 351-356, June 1974.
- [17] R. Topkaya, H. Güngüneş, Ş. Eryiğit, Sagar E. Shirsath, A. Yıldız, and A. Baykal, "Effect of bimetallic (Ni and Co) substitution on magnetic properties of MnFe₂O₄ nanoparticles," *Ceramics International*, vol. 42, iss. 12, pp. 13773-13782, September 2016.
- [18] G. Sahin, "Détermination des paramètres électriques d'une photopile à jonction verticale parallèle sous éclairage monochromatique en modulation de fréquence à partir de la caractéristique I-V," Thèse de Doctorat Unique en Physique et Applications, Faculté des Sciences et Techniques, Université Cheikh Anta Diop de Dakar, Sénégal, October 2014.
- [19] E. H. Ndiaye, G. Sahin, M. Dieng, A. Thiam, H. L. Diallo, M. Ndiaye, and G. Sissoko, "Study of the Intrinsic Recombination Velocity at the Junction of Silicon Solar under Frequency Modulation and Irradiation," *Journal of Applied Mathematics and Physics*, vol. 3, pp. 1522-1535, November 2015.
- [20] M. Sane, Z. Martial, H. L. Diallo, G. Sahin, N. Thiam, M. Diaye, M. Dieng, and G. Sissoko, "Influence of Incidence Angle on the Electrical Parameters of a vertical Silicon Solar Cell under Frequency Modulation," *International Journal of Inventive Engineering and Sciences (IJIES)*, vol. 1, iss. 11, pp. 37-40, October 2013.
- [21] M. I. Ngom, B. Zouma, M. Zougrana, M. Thiame, Z. N. Bako, A.G. Camara, and G. Sissoko, "Theoretical Study of a Parallel Vertical Multi Junction Silicon cell under Multispectral Illumination: Influence of External Magnetic Field on the Electrical Parameters," *International Journal of Advanced Technology & Engineering Research (IJATER)*, vol. 2, iss. 6, pp. 101-109, November 2012.
- [22] H. Mathieu et H. Fanet, "Physique des semi-conducteurs et des composants électroniques," 6th ed., pp. 832, Dunod, 2009.
- [23] M. Ndiaye, "Étude en régime dynamique fréquentiel d'une photopile bifaciale sous éclairage monochromatique détermination des paramètres électriques," Thèse de Doctorat 3^{ème} cycle, Université Cheikh Anta Diop de Dakar, Sénégal, 2010.
- [24] M. Santo, S. Abdelillah, K. Jean-Pa, L. Mustapha, T. Christian, L. C. Claude, D. Sebastien, M. Remi, V. Yves, P. Isabelle, L. Q. Nam, and K. Jed, "Silicon Solar Cell, Crystalline," Robert A. Meyers, Ed., *Encyclopedia of sustainability Science and Technology*, Springer Science+Business Media, LLC, Springer New York, pp. 9196-9240, 2012.

- [25] M. Erdem and C. Boyraz, "Magnetic effect on the phase properties of Neodymium activated Yttriumdisilicates nanomaterials," *Turk. J. Phys.*, DOI: 10.3906/fiz-1602-8, 2016 (in press).
- [26] T. Guven, K. Adem, and S. Erdal, "Influences of Pr and Ta doping concentration on the characteristic features of FTO thin film deposited by spray pyrolysis," *Chinese Physics B*, vol. 24, iss. 10, pp. 414-422, October 2015.
- [27] J.E. Mahan and D.L. Barnes, "Depletion layer effects in the open-circuit- voltage-decay lifetime measurement," *Solid-State Electronics*, vol. 24, iss. 10, pp. 989-994, October 1981.
- [28] T. Flohr and R. Helbig, "Determination of minority-carrier lifetime and surface recombination velocity by Optical-Beam-Induced-Current measurements at different light wavelengths," *J. Appl. Phys.*, vol. 66, iss. 7, pp. 3060-3065, 1989.
- [29] Z. Li, H. Qing, J. Wei-Long, L. Chang-Jian, and S. Yun, "Cu(In, Ga)Se₂ Thin Films on Flexible Polyimide Sheet: Structural and Electrical properties versus Composition," *Chin. Phys. Lett.*, vol. 26, no. 2, pp. 1-4, February 2009.